

REPORT DOCUMENTATION PAGE			Form Approved OMB No. 0704-0188	
<p>Public reporting burden for this collection of information is estimated to average 1 hour per response, including the time for reviewing instructions, searching existing data sources, gathering and maintaining the data needed, and completing and reviewing this collection of information. Send comments regarding this burden estimate or any other aspect of this collection of information, including suggestions for reducing this burden to Department of Defense, Washington Headquarters Services, Directorate for Information Operations and Reports (0704-0188), 1215 Jefferson Davis Highway, Suite 1204, Arlington, VA 22202-4302. Respondents should be aware that notwithstanding any other provision of law, no person shall be subject to any penalty for failing to comply with a collection of information if it does not display a currently valid OMB control number. PLEASE DO NOT RETURN YOUR FORM TO THE ABOVE ADDRESS.</p>				
1. REPORT DATE (DD-MM-YYYY) May 2012		2. REPORT TYPE Technical Paper		3. DATES COVERED (From - To) May 2012-July 2012
4. TITLE AND SUBTITLE Moment Preserving Adaptive Particle Weights using Octree Velocity Distributions for PIC Simulations			5a. CONTRACT NUMBER In-House	
			5b. GRANT NUMBER	
			5c. PROGRAM ELEMENT NUMBER	
6. AUTHOR(S) Robert Scott Martin and Jean-Luc Cambier			5d. PROJECT NUMBER	
			5e. TASK NUMBER	
			5f. WORK UNIT NUMBER 23041057	
7. PERFORMING ORGANIZATION NAME(S) AND ADDRESS(ES) Air Force Research Laboratory (AFMC) AFRL/RQRS 1 Ara Drive. Edwards AFB CA 93524-7013			8. PERFORMING ORGANIZATION REPORT NO.	
9. SPONSORING / MONITORING AGENCY NAME(S) AND ADDRESS(ES) Air Force Research Laboratory (AFMC) AFRL/RQR 5 Pollux Drive Edwards AFB CA 93524-7048			10. SPONSOR/MONITOR'S ACRONYM(S)	
			11. SPONSOR/MONITOR'S REPORT NUMBER(S) AFRL-RZ-ED-TP-2012-211	
12. DISTRIBUTION / AVAILABILITY STATEMENT Distribution A: Approved for Public Release; Distribution Unlimited. PA#12553				
13. SUPPLEMENTARY NOTES Conference paper for the 28th International Symposium on Rarefied Gas Dynamics, Zaragoza, Spain, 9-13 July 2012.				
14. ABSTRACT The ratio of computational to physical particles is of primary concern to statistical particle based simulations such as DSMC and PIC. An adaptive computational particle weight algorithm is presented that conserves mass, momentum, and energy. This algorithm is then enhanced with an octree adaptive mesh in velocity space to mitigate artificial thermalization. The new octree merge is compared to a merge that randomly selects merge partners for a bi-Maxwellian velocity distribution. Results for crossing beams in a fixed potential well along with an electrostatic PIC version with and without MCC collisions based ionizing breakdown show the advantages of the merge algorithm to both fixed particle weights and randomly selected merge partners.				
15. SUBJECT TERMS				
16. SECURITY CLASSIFICATION OF:			17. LIMITATION OF ABSTRACT SAR	18. NUMBER OF PAGES 41
a. REPORT Unclassified	b. ABSTRACT Unclassified	c. THIS PAGE Unclassified		
				19b. TELEPHONE NO (include area code) 661-275-5649

Moment Preserving Adaptive Particle Weights using Octree Velocity Distributions for PIC Simulations

Robert Scott Martin* and Jean-Luc Cambier[†]

**ERC Inc.,*

*[†]Spacecraft Propulsion Branch,
Air Force Research Laboratory,
Edwards AFB, CA 93524 USA*

Abstract. The ratio of computational to physical particles is of primary concern to statistical particle based simulations such as DSMC and PIC. An adaptive computational particle weight algorithm is presented that conserves mass, momentum, and energy. This algorithm is then enhanced with an octree adaptive mesh in velocity space to mitigate artificial thermalization. The new octree merge is compared to a merge that randomly selects merge partners for a bi-Maxwellian velocity distribution. Results for crossing beams in a fixed potential well along with an electrostatic PIC version with and without MCC collisions based ionizing breakdown show the advantages of the merge algorithm to both fixed particle weights and randomly selected merge partners.

Keywords: Particle Merge, Particle in Cell, PIC, Adaptive Methods, MCC

PACS: 51.xxxxx

INTRODUCTION

The ratio of computational to physical particles is a key factor in determining the statistical scatter and accuracy in particle-based simulation. This is particularly true for problems characterized by wide ranges of number density such as those found in spacecraft electric propulsion plumes and ionizing discharges, where populations of electrons and excited states can grow exponentially. A particle management method must then be devised which balances statistical accuracy requirements with prevention of runaway computational costs.

The standard approach of merging of particles[1] using pair-wise coalescence (2:1 ratio), cannot guarantee simultaneous conservation of mass, momentum and energy. The pair-wise coalescence conserves mass by simply summing the computational weight of the individual constituents. One computational particle only has three degrees of freedom for velocity. The resulting particle can therefore either match the average momentum or the kinetic energy of the original pair, but never both simultaneously. The growth of this error is limited by selecting particles that are near each other in velocity space, but is a fundamental consequence of the reduction of degrees of freedom.

As a result of this inherent limitation, various sophisticated models have been designed to mitigate the error in momentum or energy. Hewett used computational particles with internal energy in which the error could be accumulated[2]. Assous and then Welch designed methods of merging values to grid nodes and redistributing the moments to particles[3, 4]. Though exact energy and momentum conservation is possible with these methods, they are considerably more complicated than the original naive 2:1 merge.

MOMENT PRESERVING MERGE

Having identified the lack of sufficient degrees of freedom in the merge resultant particle as the source of the error, Cambier devised a simple method[5] which relies on the generation of a pair of particles. The particle pair provides the required freedom to conserve all moments up to 2nd order exactly. The pair of resultant particles have the same mean momentum as the originals, but they also have equal and opposite components of velocity perpendicular to the mean

momentum such that energy is conserved. The moments to be conserved are shown in Equation 1. In these equation, the ' k ' original particles, denoted with superscript ' (p) ', and the bar denotes an average quantity used in the Merge. The subscripts denote the vector direction whether index, i , or directions parallel or perpendicular. Assuming the pair of merge result particles are equal weight, the formulas for the merge can be seen in Equation 2 where superscript ' (a/b) ' refers to one or the other of the merge result particles. It can be shown that the moment sums are equivalent between the k original and pair of resultant particles. Thus, pair-wise reduction is obtained through an equivalent ratio of 4:2. These formulas also work for arbitrary ratios $(n+2):2$ with the same conservation properties.

$$\bar{m} = \sum_p^k m^{(p)} \quad (1)$$

$$\bar{v}_i = \frac{\sum_p^k m^{(p)} v_i^{(p)}}{\sum_p^k m^{(p)}}$$

$$\overline{v_i^2} = \frac{\sum_p^k m^{(p)} \left(v_i^{(p)} - \bar{v}_i \right)^2}{\sum_p^k m^{(p)}}$$

$$m^{(a/b)} = \bar{m}/2 \quad (2)$$

$$v_{||} = v_{i,cm} = \bar{v}_i$$

$$v_{\perp} = \sqrt{\overline{v_i^2}}$$

$$v_i^{(a/b)} = v_{||} \pm v_{\perp}$$

It is important to note that in this example, some ambiguity in the sign of perpendicular velocity component remains. For the purposes of this work, each cardinal direction is randomly assigned a sign for one of the particles and the second particle uses the opposite sign in each direction. As a result of this choice of signs, though the component of temperature is conserved in each direction independently, though the choice is not unique and particles may scatter perpendicular to a dominant axis of the distribution. A better choice would be to determine the sign of mixed second order moments and use that to assign the signs for the particle. If for example, most of the particles lay on the $(-x, -y, -z) \rightarrow (+x, +y, +z)$ line, the sign of the mixed moments would all be positive and all of the particle signs should match. However, this approach is left to future consideration along with higher moment conservation in extension and conclusion section.

Though this merge exactly conserves the moments through energy, it can result in artificial thermalization of the velocity distribution. This is easily seen by considering the result of merging particles from two mono-energetic beams of opposite direction. Though the energy of the resulting velocity distribution would be unchanged, the merge results in a range of particles scattered throughout the gap between and outside the original beams. For example, if two equal mass particles were selected from the $+v$ side beam and a third of equal mass from the $-v$ side, the mean velocity would be at $+v/3$ and the resulting particle velocities would be symmetric $v/3 \pm \sqrt{24/27} v$ and therefore clearly not back into the original $+v$ and $-v$ beams.

OCTREE ADAPTIVE MESH

The present work extends this exact moment-preserving merge through an octree-based adaptive mesh in velocity space to ensures that merging partners are relatively close in phase space. This mitigates artificial thermalization due to merging of particles with large opposite velocities such as those found in the beam-beam interaction example. Rather than randomly selecting merge partners, the particles are first sorted into octants of velocity space. Each of these octants is then recursively subdivided and the particles are sorted into the sub-cells. The recursion was originally terminated once the number of particles in a given sub-cell is below a specified threshold. The conservative merge is then applied to the particles within one velocity space sub-cell.

To test the modified octree based conservative merge, a bi-Maxwellian velocity distribution was used. Figure 1 contrasts results from a randomly selected 4:2 merge and the octree based (3-11):2 based merge where (3-11) refers to the range of computational particles per sub-cell to be merged. In the example shown, the random merge resulted in a reduction of 10,000 \rightarrow 5,000 computational particles while the octree merge starts with the original particles and performs a reduction of 10,000 \rightarrow 4,727.

The threshold was set to 11-particles per sub-cell because it was found to result in a net merge ratio of approximately 2:1. This is lower than 5.5:1 because, in each of the eight children cells, the number of particles ranges between 0-11 rather than being exactly 11 particles. For example, cells with fewer than three particles cannot be conservatively merged at all. The effective merge was found heuristically to result in approximately 2:1 reduction had 11 as the upper

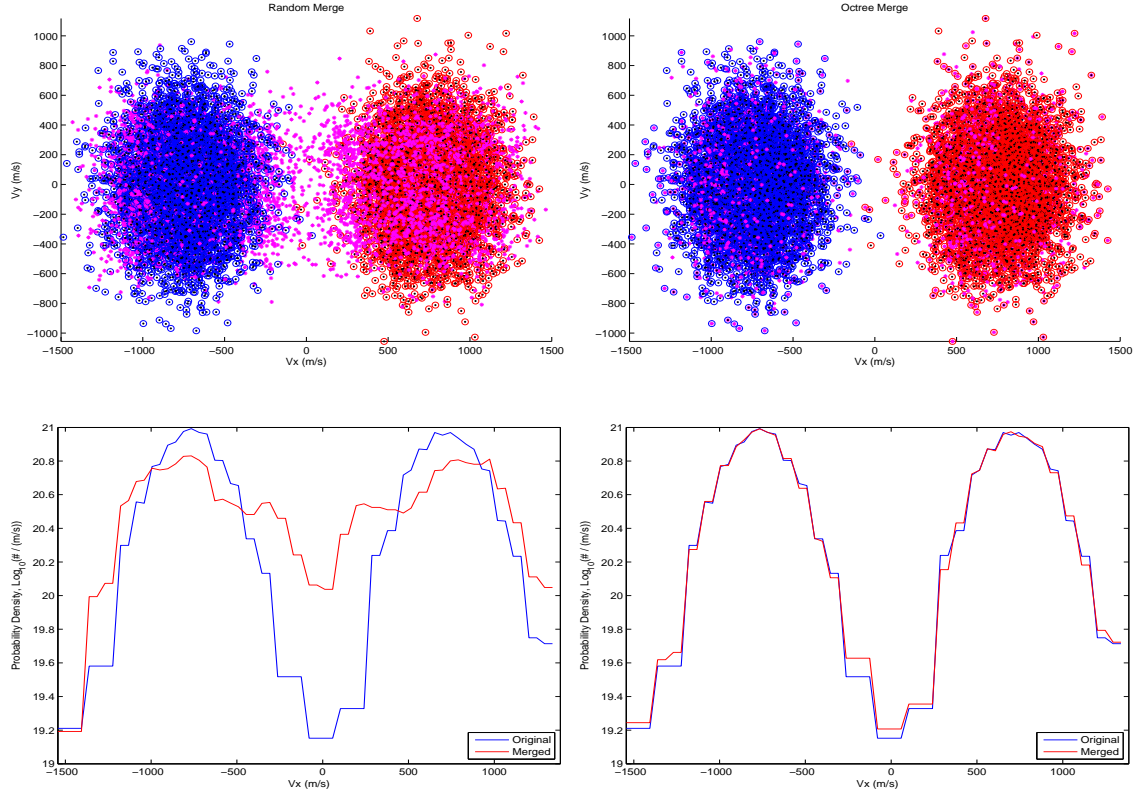


FIGURE 1. Comparison of randomly selected 4:2 merge (left) and octree based (3-11):2 merge (right). The scatter plots (top) show particle positions in velocity space and the line plots (bottom) compare the original and merged velocity distributions integrated over y - and z -velocity. In the scatter plots, the original particles are marked by the black dots, the left and right halves of the original bi-Maxwellian are circled with blue and red respectively, and the output merged particles are marked in violet.

limit. This ratio may be problem dependent and should therefore be considered a tunable parameter that quantifies the aggressiveness of the merging procedure rather than as a direct prescription for a specific merge ratio.

For fully adaptive particle weights, an analogous particle split method is necessary to re-populate depleted velocity distributions that result from the particle merging. Without this split, particles merged when the spatial distribution is compact result in extremely noisy values as the distribution expands. The split is achieved by performing operations using the conservative moment sums similar to those of the merge. Instead of consuming the entire original particles to form the merge results, only a fraction of each original particle is consumed to form the new pair. The effective split has a ratio of $(n+2):(n+2+2)$. This approach only offers a weak growth in the number of computational particles. Instead, subsets of 3-4 particles are selected from the particles residing in the particular velocity sub-cell in which the split operation is being performed. For each of these subsets, a 3:5 or 4:6 split is performed yielding a higher computational particle growth rate. This split technique is used in the results presented.

In later studies with DSMC collisions, low density regions were populated by collision events that scattered velocity out of the original distributions. Repeated merging as particles scattered out of the core of the distribution resulted in a depletion of computational particle number within the core in favor of a few heavy particles. To compensate for this trend, the cell merge limit was modified such that cells are only subdivided when the total weight of particles within the cell exceed a target weight. This target weight can then be modified for each cell so that the merge procedure attempts to achieve a uniform number of computational particles per cell and therefore computational work.

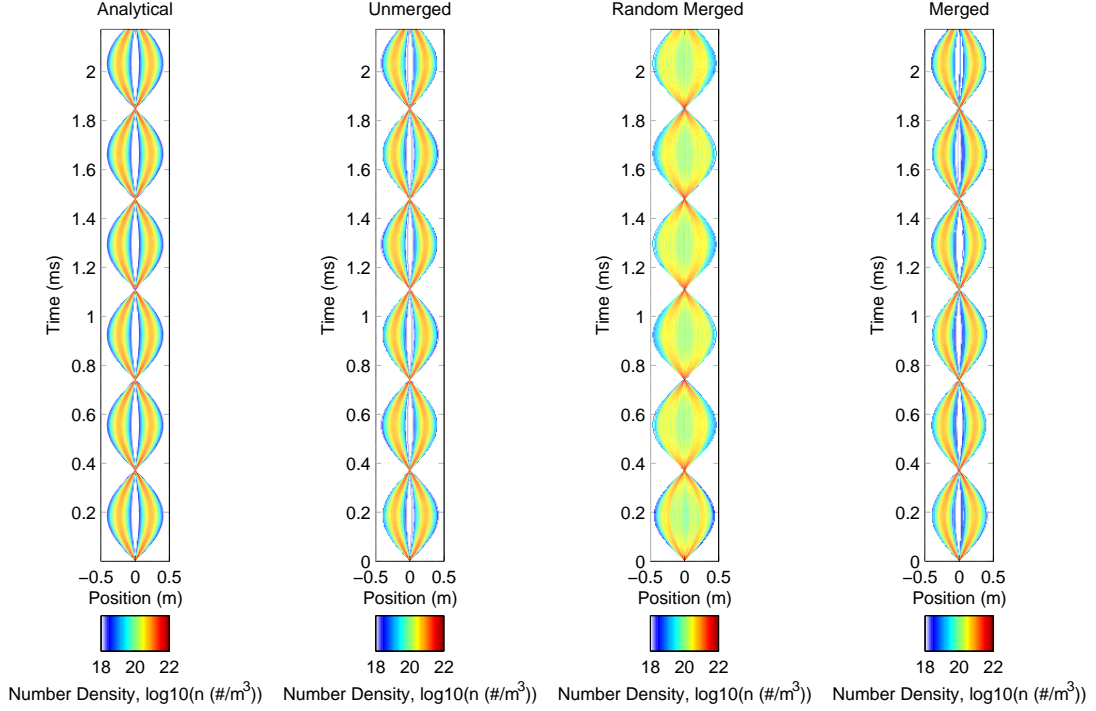


FIGURE 2. Position vs Time results of particle number density for Analytical, Fixed Weight, Random 4:2 Merge, and Octree based Merge.

POTENTIAL WELL TEST CASES

The combined fully-adaptive particle weighting scheme can now be applied to several test-problems. The first is collisionless thermal beams in a potential well. The initial conditions consist of a bi-Maxwellian distribution of particles at the center on a fixed parabolic potential well. The two halves of the bi-Maxwellian initially separate in opposite directions. The acceleration due to the electric field then decelerates the particles and they fall back across the bottom of the well. They then proceed to the opposite side of the well and continue oscillating indefinitely.

This setup is a particularly useful surrogate for the expansion of a plasma plume because the particle density falls off by several orders of magnitude between the center and edges of the well. It is also useful because an exact analytical solution can be derived for the evolution of the density profile as follows.

In this simple invariant potential well setup, every particle in the initial distribution follows a simple oscillatory trajectory such that the sum of kinetic and potential energies is constant. It can then be shown that the position and velocity for each particle follows the sinusoidal trajectory based on the initial velocity and position.

The trajectories can then be solved for the initial velocities for particles between the 'inner' and 'outer' edges of a spatial cell at any time of interest. These inner and outer velocities can then be used as the lower and upper limits of integration on the initial bi-Maxwellian velocity distribution to determine the number of particles within a cell at a given time.

For the particle simulations, an implicit Crank-Nicolson particle push using the analytically defined parabolic potential was used. This push was selected due to its exact marginal stability and energy conservation properties for simple harmonic oscillation. This allows the simulation to run for several beam oscillations without numerical heating or cooling. The timesteps were selected based on a CFL criteria such that the fastest particles in the original distribution only cross a single computational cell in a timestep.

Figure 2 shows number density results for the Analytical, Fixed Particle Weight, Randomly Selected 4:2 Merge, and Octree Merge. Clearly the results for Octree Merged and Fixed particle weights are quite similar and match the analytical results across the 4-orders of magnitude in particle density depicted.

This problem explicitly highlights the disadvantage of the random merge partner selection in thermalizing the distribution. The thermalization occurs in the first timestep when the particles all reside in the central cell with opposite

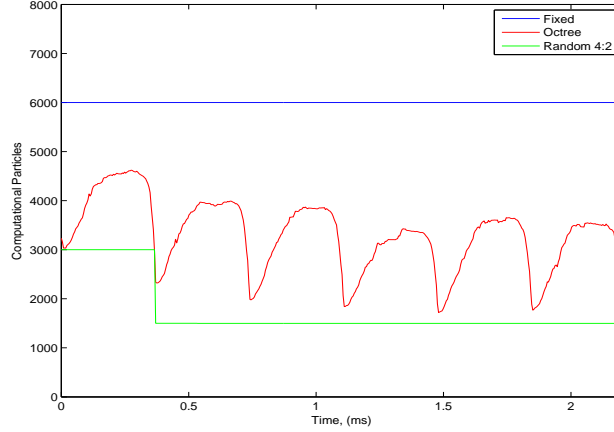


FIGURE 3. Comparison of number of computational particles throughout the simulations for Fixed Weight, Random 4:2 Merge, and Octree based Merge.

directions. The random selection mixes particles from opposite sides of the initial bi-Maxwellian distribution and fills in the center. Even though the figure looks dramatically different, all of the moments are conserved in each cell. For every particle that lost momentum and energy to fill in the center figure, others gained momentum and energy which results in a wider fringe.

Figure 3 shows the number of computational particles for the different particle management techniques. All of the cases started with the same 6000 computational particles. The figure shows that the initial merge between the random and octree techniques are of similar magnitude despite the dramatic difference in the density plots. The random merge technique also does not include a split and so the number of particles monotonically decreases in steps with the bounce frequency.

SPARK GAP TEST CASE

A second test of the merging algorithm involves electron avalanche in a spark gap gas breakdown. The simulation is initialized with a 6kV potential drop across a 5mm gap. In this example, the particles tracked are the electrons in a partially ionized background Argon gas which is assumed stationary for the duration of the simulation.

The 1-D code was modified to include the effect of the charge distribution on the electrostatic potential. The charge density ρ , was assumed constant within the cell and was simply the difference of electron and ion densities multiplied by the fundamental electron charge. Control points for a quadratic b-spline were then solved for the potential from the charge density such that $\nabla^2\Phi = -\rho$. The boundary conditions of $\pm 3\text{kV}$ were also applied to the solution of the control points. Electrons that arrived at the $+3\text{kV}$ boundary were re-injected at the -3kV boundary with a small thermal velocity to maintain charge neutrality. The injected particles were injected randomly in the inside half of the boundary cell so that self-forcing due to the 0D-representation of the charge density does not cause the particles to be pushed back out of the domain. Though this is only a rough representation of an electrostatic PIC model, it is sufficient for testing the octree merge algorithms.

In addition to the modifications to the potential for the spark gap case, the push was modified to an analytical form rather than using Crank-Nicolson. Because the potential is represented by a piecewise quadratic b-spline, the electric field is a piecewise linear continuous function. The exact solution for a particle undergoing an acceleration that depends linearly on position, $\vec{a} = \frac{q}{m}\vec{E} = \frac{q}{m}[\vec{E}_0 + \frac{\partial\vec{E}}{\partial\vec{x}}|_{x_0}(\vec{x} - \vec{x}_0)]$, can easily be found in 1D. It has the form shown in Equation 3 with constants defined in Equation 4. The equation assumes a piecewise-linear electric field and is therefore only valid within one computational cell.

$$x(t) = -\frac{C_1}{\sqrt{\lambda}}e^{-\sqrt{\lambda}t} + \frac{C_2}{\sqrt{\lambda}}e^{\sqrt{\lambda}t} - \frac{qE_0}{\lambda} \quad v(t) = C_1e^{-\sqrt{\lambda}t} + C_2e^{\sqrt{\lambda}t} \quad (3)$$

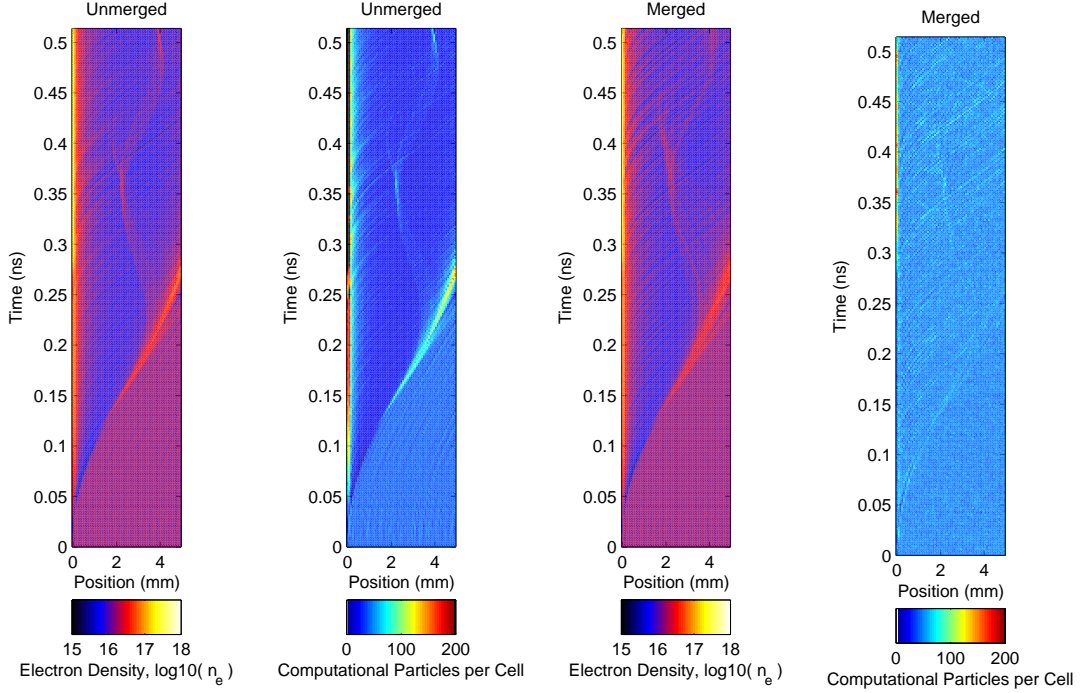


FIGURE 4. Position vs Time results of electron density and computational particles per cell in spark gap. Electrons are pushed from the cathode on the left to anode on the right of the figures due to the 6kV applied potential. The left figure shows the original electron density with fixed particle weight and the right figure shows the electron density for the octree merge algorithm.

$$C_1 = -\left(x_0\sqrt{\lambda} - v_o + \frac{q}{m}E_0\right)/2 \quad C_2 = \left(x_0\sqrt{\lambda} + v_o + \frac{q}{m}E_0\right)/2 \quad \lambda = \frac{q}{m} \frac{\partial E}{\partial x} \Big|_{x_o} \quad (4)$$

To account for the change of slope at cell boundaries, the cell boundary crossing times are found and particles are pushed only within one cell at a time. The time at which a particle crosses x_0 or $x_0 + \Delta x$ can then be solved by substituting $x(t) = x_0$ or $x_0 + \Delta x$ and $\alpha = e^{\sqrt{\lambda}t}$ into the formula for $x(t)$ and solving the quadratic equation for α . The crossing times for the cell edges are then simply $t = \sqrt{\lambda} \ln(\alpha)$. Note that each side has two possible α -s as roots of the quadratic equation. The set of four crossing times may then each be positive, negative, or imaginary. Each particle is then advanced by the smallest real positive time or full timestep if shorter using Equation 3 repeatedly until the full timestep is complete. The full timestep is based on a CFL condition assuming an electron accelerated by a 6kV potential cannot cross more than one cell per timestep.

In the test case, the background was initialized at 0.1% singly charged ionization in a $1e22/m^3$ background of Argon. The evolution of the electron density is shown in Figure 4. An interesting feature is the oscillation of trapped electrons that are pulled back from the initial acceleration. This feature is a result of the potential exceeding the anode boundary condition in the positive column followed up to the anode sheath. The slowest electrons that have insufficient kinetic energy to overcome the sheath voltage fall back towards the cathode and oscillate indefinitely because the plasma is collisionless. This example is quite similar to the crossing beams in the potential well of the previous example and again demonstrate the importance of the octree merge's minimal thermalization.

In addition to the modified particle push, a simple inelastic MCC collision process was added between the electrons and background gas. The energy dependent cross section used was based off the data in Reference[6] using the form given in Equation 5. In the equation, C is the slope of cross-section vs energy above the ionization threshold energy, I . The maximum cross section, σ_{max} is the peak cross section prior to a further reduction with increasing collision energy. For Argon, values of $C = 2e-17cm^2/ev$, $I = 15.8ev$, and $\sigma_{max} = 3.7e-16cm^2$ from Reference [6] were also used to approximate the electron impact ionization cross section. For this sample problem, all other collision types including Coulomb and recombination collisions were ignored.

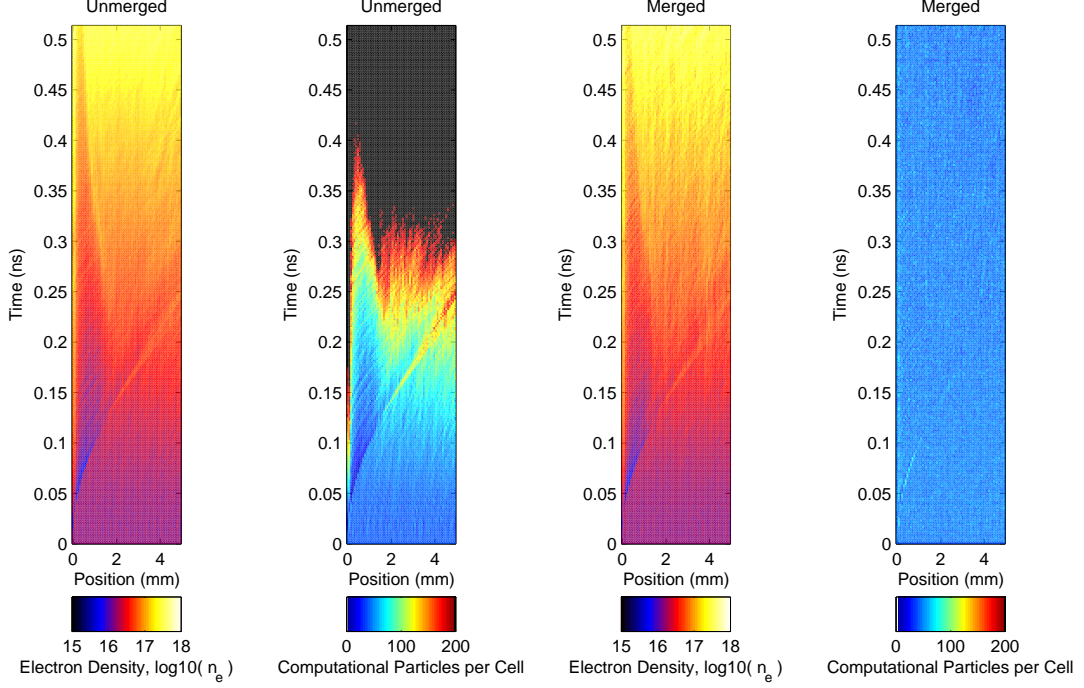


FIGURE 5. Position vs Time diagram of electron density and computational particles per cell in an ionizing spark gap using MCC collision model. Electrons are pushed from the cathode on the left to anode on the right of the figures due to the 6kV applied potential. The left two figure shows the original electron density and computational particles per cell with fixed particle weights and the right two figure shows the same results using the octree merge algorithm.

$$\sigma(e) = \min(C(e - I), \sigma_{max}) \quad (5)$$

Based on the collision frequency from the cross section, particles are selected to either undergo collision with the background gas or not. If a particle is selected for collision, it's kinetic energy is reduced by the ionization potential, I , and a new electron of equal computational weight is created with zero velocity at the same location. The background neutral density is also decreased by the same weight so that the ion density can be determined as $n_i = n_0 - n_n$.

With the addition of MCC ionization collisions, the growth of the number of computational electrons is exponential from a small initial ionization fraction. This is exactly the type of situation for which the merge algorithm was designed. Without the ability to adaptively adjust particle weights throughout the simulation, the computational cost rapidly exceeds the resources available even if only a few and therefore statistically inaccurate seed electrons are initialized.

Finally, Figure 6 shows the total number of particles for the fixed weight and octree merged MCC ionizing breakdown case. The particle weight adaptation is clearly compensating for what would otherwise be an exponential growth in computational particles. Though the density results are noisier, this should be expected for few degrees of freedom in the system. The key feature is that the computational cost is now decoupled from particle weight using the octree based particle merge.

FUTURE EXTENSION AND CONCLUDING REMARKS

The issue of mixed second order moments mentioned previously ties into the concept of extending the conservative merge to higher moments of the velocity distribution. Using index notation, it is clear that current formulation conserves one 0th order moment for the mass, \bar{m} , three 1st order moments for velocity \bar{v}_i , and three diagonal 2nd order moments $\bar{v}_i \bar{v}_i$. In the typical notations of the moments in statistical mechanics, it is useful to define these moments instead in terms of the peculiar velocity of the particles, $V_i = v_i - \bar{v}_i$. The diagonal second order moment is then simply proportional to the diagonal terms of the pressure tensor, $P_{ij} = nm \overline{V_i V_j}$ as defined in Reference [7]. Though the net

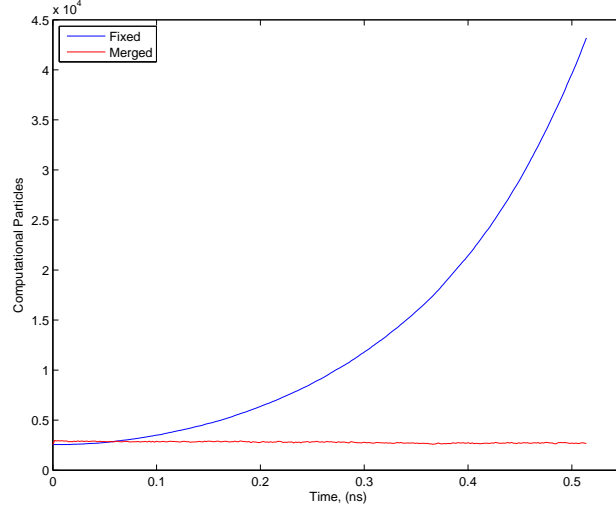


FIGURE 6. Comparison of number of computational particles throughout the ionizing breakdown for Fixed Weight and Octree Merge.

thermal energy, $\overline{V_i V_i}$ is conserved, each component of $\overline{V_i V_i} = \overline{V_x V_x} + \overline{V_y V_y} + \overline{V_z V_z}$ is also conserved independently. This allows for anisotropic pressure/temperature, but makes no guarantee that shear stress is conserved.

Adding a third product particle to the merge procedure with the constraint that all three product particle masses are equal provides sufficient degrees of freedom to satisfy conservation of the full second order moment, $\overline{V_i V_j}$. Though it would appear that there are 6-additional moments for the full second order tensor, the moment integral is commutative for $\overline{V_i V_j} = \overline{V_j V_i}$ and therefore the three additional degrees of freedom are sufficient. However, these additional degrees of freedom no longer allow for direct solution and require a non-linear solve for the merge result velocities.

Similarly, adding a fourth particle adds the ability to conserve $\overline{V_i V_j V_j}$. This is equivalent to conserving the heat flux vector, and is sufficient to conserve the 13-moments necessary to the Navier-Stokes solution to the Chapman-Enskog expansion without the restriction of isotropy. Work has begun to solve for the set of four particle velocities that result in the correct moments using a Newton-Raphson style non-linear solver. The solution requires stabilization due to saddle points in the 12-dimensional solution space. Further work to extend this method to solve on the energy constrained manifold is hoped to alleviate these issues. Developing a merge routine to this level would be potentially useful in developing hybrid particle/continuum codes.

Along with these velocity moments, spatial moments can be similarly conserved and are necessary for conserving electrostatic potential energy during the merge as developed in the original development of the conservative merge algorithm [5]. In addition, future work will include consideration of conservation of magnetic moments and internal energy.

These merging and splitting algorithms show tremendous promise for future particle codes that involve strong particle growth and/or large dynamic range in particle density. They also provide the groundwork for modified collision routines that are not constrained to constant numbers of computational particles as discussed in the accompanying paper, Reference [8].

REFERENCES

1. G. Lapenta, and J. U. Brackbill, *Journal of Computational Physics* **115**, 213 – 227 (1994).
2. D. W. Hewett, *Journal of Computational Physics* **189**, 390 – 426 (2003).
3. F. Assous, T. P. Dulimbert, and J. Segré, *Journal of Computational Physics* **187**, 550 – 571 (2003).
4. D. Welch, T. Genoni, R. Clark, and D. Rose, *Journal of Computational Physics* **227**, 143 – 155 (2007).
5. J.-L. Cambier, AFOSR computational mathematics program contractor's review (2006).
6. Y. B. Zel'dovich, and Y. Raizer, *Physics of Shock Waves and High-Temperature Hydrodynamic Phenomena*, Dover, 2002.
7. J. Hirschfelder, *Molecular Theory of Gases and Liquids*, John Wiley & Sons, New York, 1954.
8. R. Martin, and J.-L. Cambier, "Low Noise Fractional NTC Collisions for DSMC," 2012.

MOMENT PRESERVING ADAPTIVE PARTICLE WEIGHTS USING OCTREE VELOCITY DISTRIBUTIONS FOR PIC SIMULATIONS

Robert Martin & Jean-Luc Cambier

ERC INC.,
SPACECRAFT PROPULSION BRANCH
AIR FORCE RESEARCH LABORATORY
EDWARDS AIR FORCE BASE, CA USA



28th International Symposium on Rarefied Gas Dynamics





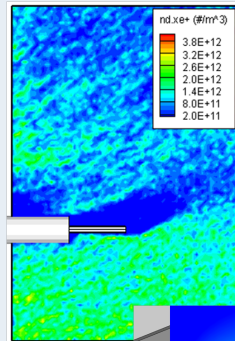
- 1 BACKGROUND
- 2 CONSERVATIVE PARTICLE MERGING
- 3 RESULTS
- 4 FUTURE EXTENSIONS



Spacecraft Propulsion Relevant Plasmas:

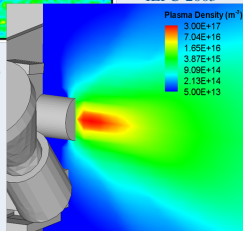
- Plumes from hall thrusters
- Discharge and Breakdown in FRC
- Relevant Densities can Span 6+ Orders of Magnitude
- Good Statistics in Plume Requires Computationally Prohibitive Particle Numbers in Engine

Electric Propulsion Plumes



Fife et. al.,
IEPC-2003

Brieda et. al.,
AIAA-2006-5023





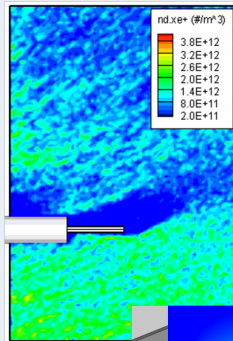
Spacecraft Propulsion Relevant Plasmas:

- Plumes from hall thrusters
- Discharge and Breakdown in FRC
- Relevant Densities can Span 6+ Orders of Magnitude
- Good Statistics in Plume Requires Computationally Prohibitive Particle Numbers in Engine

Solution?

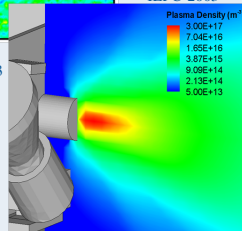
Adaptive Physical:Computational Weights

Electric Propulsion Plumes



Fife et. al.,
IEPC-2003

Brieda et. al.,
AIAA-2006-5023





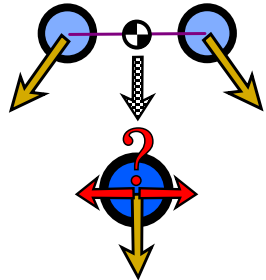
PRIOR MERGING TECHNIQUES

Numerous Previous Merge Methods:



Numerous Previous Merge Methods:

- 2:1 - Cannot Conserve Energy
(Lapenta & Brackbill, JCP 1994)

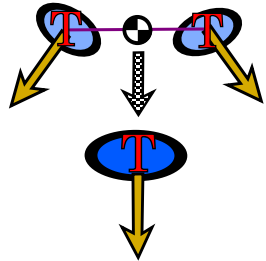




PRIOR MERGING TECHNIQUES

Numerous Previous Merge Methods:

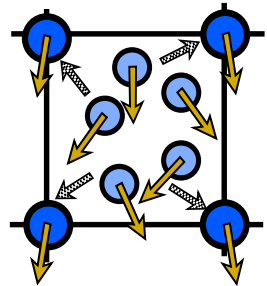
- 2:1 - Cannot Conserve Energy
(Lapenta & Brackbill, JCP 1994)
- Complex Macro-particles with Internal Energy
(Hewett, JCP 2003)





Numerous Previous Merge Methods:

- 2:1 - Cannot Conserve Energy
(Lapenta & Brackbill, JCP 1994)
- Complex Macro-particles with Internal Energy
(Hewett, JCP 2003)
- Merge to Grid
(Assous et al., JCP 2003, Welch et al., JCP 2007)

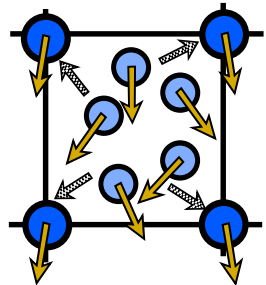




Numerous Previous Merge Methods:

- 2:1 - Cannot Conserve Energy
(Lapenta & Brackbill, JCP 1994)
- Complex Macro-particles with Internal Energy
(Hewett, JCP 2003)
- Merge to Grid
(Assous et al., JCP 2003, Welch et al., JCP 2007)

All Introduce Significant Error and/or Complexity



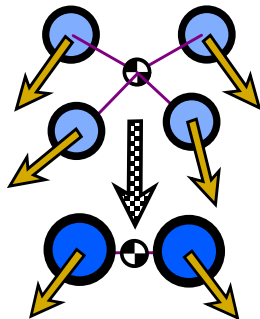


CONSERVATIVE MERGE

Merge to Pair \rightarrow DOF for Conservation:

- $(n+2):2$ yields Exact Mass, Momentum, and Kinetic Energy Conservation
- Applied Spatially also Shown to Conserve Electrostatic Energy
- Though Energy Conserving, Still Thermalizes VDF

(Cambier, AFOSR Review 2006)





CONSERVATIVE MERGE

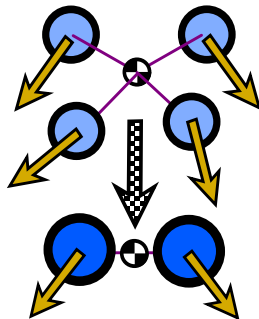
Merge to Pair → DOF for Conservation:

- $(n+2):2$ yields Exact Mass, Momentum, and Kinetic Energy Conservation
- Applied Spatially also Shown to Conserve Electrostatic Energy
- Though Energy Conserving, Still Thermalizes VDF

(Cambier, AFOSR Review 2006)

Selection of Near Neighbors in VDF Limits Thermalization

(Like Near Neighbor Selection in Advanced 2:1 Merges to Limit Numerical Cooling)





OCTREE MERGE

Advantages of Octree Sort:

- Octree Prevents Merge Across Distribution
- Limits Thermalization
- Conserves Entropy up to Octree Quadrature

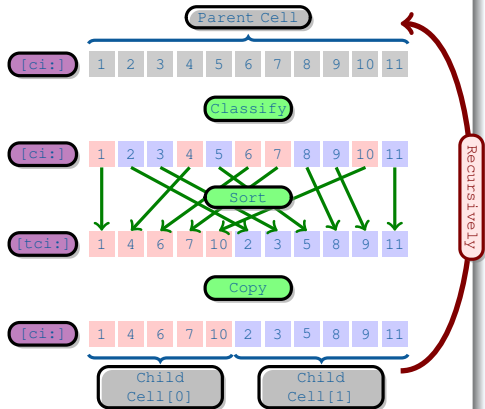
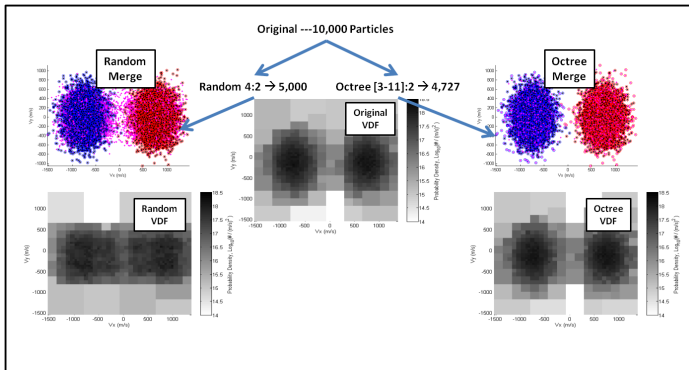


FIGURE: Cell Index Particle Sorting Procedure



0D-MERGE EXAMPLES

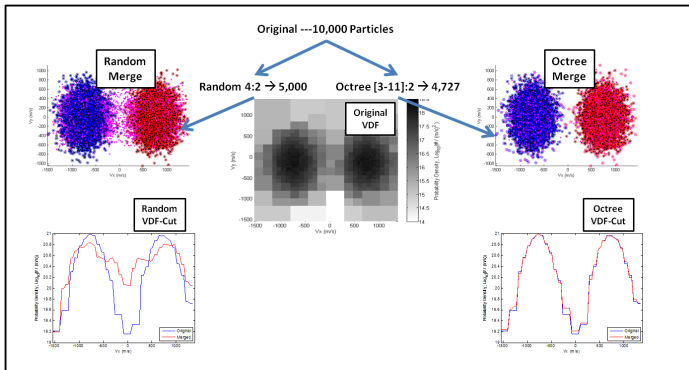
Comparison of Random vs. Octree Merge Partner Selection (Note: Mass, Momentum, and Kinetic Energy Both Exactly Conserved)





0D-MERGE EXAMPLES

Comparison of Random vs. Octree Merge Partner Selection (Note: Mass, Momentum, and Kinetic Energy Both Exactly Conserved)

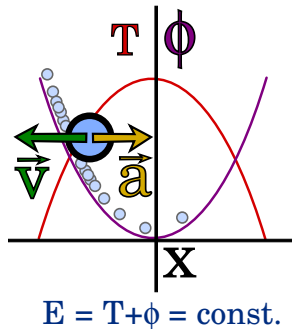




BEAM IN POTENTIAL WELL

Collisionless Crossing Beams:

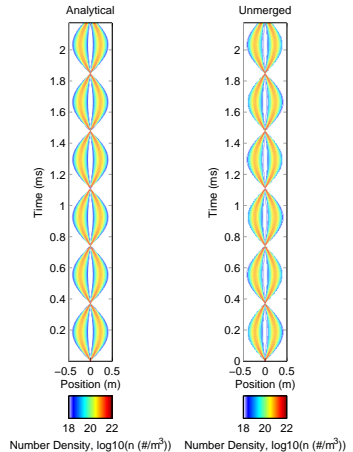
- Particles in Parabolic Potential Well
- Constant Potential
- Collisionless \rightarrow Known Trajectory, $x(t)$
- Sinusoidal Path from Initial Velocity
- Analytical Solution for Density, $n(x, t)$
- Crank-Nicolson Particle Simulations
- C-N is Stable and Non-Dissipative for $\text{Re}(\lambda)=0$





BEAM IN POTENTIAL WELL

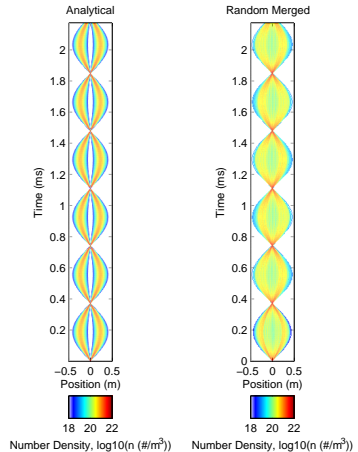
- 6000 Unmerged Particles
- Reproduces 3-4 Orders of Magnitude





BEAM IN POTENTIAL WELL

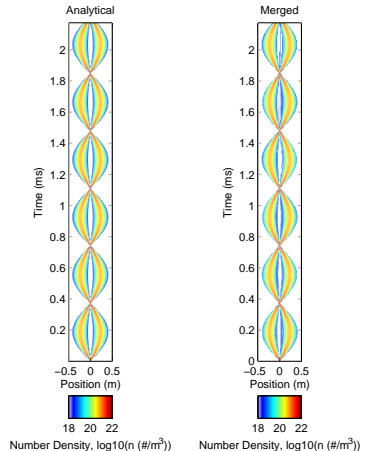
- 6000 Unmerged Particles
- Reproduces 3-4 Orders of Magnitude
- Random Merge -> Thermalization
- 3000 First Point, 1500 First Cross
- Bi-Maxwellian Specifically Difficult





BEAM IN POTENTIAL WELL

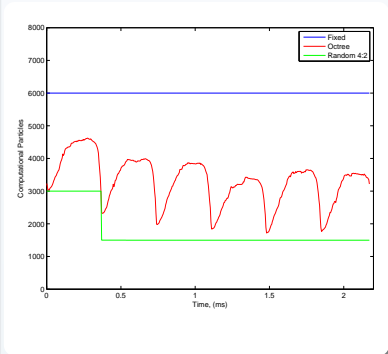
- 6000 Unmerged Particles
- Reproduces 3-4 Orders of Magnitude
- Random Merge -> Thermalization
- 3000 First Point, 1500 First Cross
- Bi-Maxwellian Specifically Difficult
- Octree Merge Significantly Better





BEAM IN POTENTIAL WELL

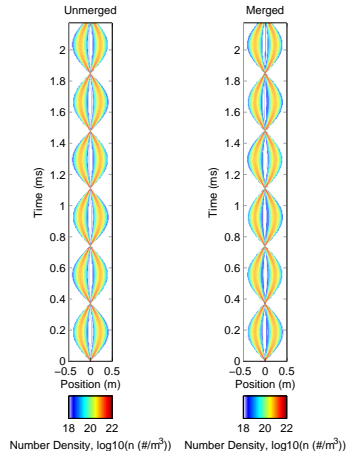
- 6000 Unmerged Particles
- Reproduces 3-4 Orders of Magnitude
- Random Merge -> Thermalization
- 3000 First Point, 1500 First Cross
- Bi-Maxwellian Specifically Difficult
- Octree Merge Significantly Better
- Merge & Split Adapts Particle Count





BEAM IN POTENTIAL WELL

- 6000 Unmerged Particles
- Reproduces 3-4 Orders of Magnitude
- Random Merge -> Thermalization
- 3000 First Point, 1500 First Cross
- Bi-Maxwellian Specifically Difficult
- Octree Merge Significantly Better
- Merge & Split Adapts Particle Count
- Despite Continuous Weight Scaling, Similar Results over Several Bounces





GAS BREAKDOWN

- Merge Needed w/ Exponential # Growth



GAS BREAKDOWN

- Merge Needed w/ Exponential # Growth
- Examples...

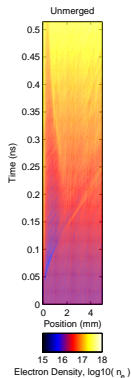
Chain Branching: $\text{H}_2 + \text{M} \rightarrow 2\text{H} + \text{M}$

Ionization: $\text{Ar}^0 + e^- \rightarrow \text{Ar}^+ + e^- + e^-$



GAS BREAKDOWN

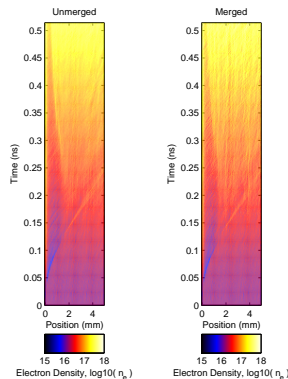
- Merge Needed w/ Exponential # Growth
- Examples...
 - Chain Branching: $\text{H}_2 + \text{M} \rightarrow 2\text{H} + \text{M}$
 - Ionization: $\text{Ar}^0 + e^- \rightarrow \text{Ar}^+ + e^- + e^-$
- Ionizing Breakdown in 6kV Potential
- Electrons Flow from Cathode \rightarrow Anode
- Inelastic MCC with Background
- Potential Function of e^- and Ar^+





GAS BREAKDOWN

- Merge Needed w/ Exponential # Growth
- Examples...
 - Chain Branching: $\text{H}_2 + \text{M} \rightarrow 2\text{H} + \text{M}$
 - Ionization: $\text{Ar}^0 + e^- \rightarrow \text{Ar}^+ + e^- + e^-$
- Ionizing Breakdown in 6kV Potential
- Electrons Flow from Cathode \rightarrow Anode
- Inelastic MCC with Background
- Potential Function of e^- and Ar^+
- Merge Retains Features and Magnitude

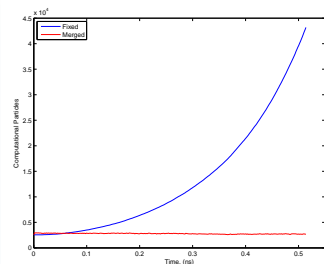




GAS BREAKDOWN

- Merge Needed w/ Exponential # Growth
- Examples...
 - Chain Branching: $\text{H}_2 + \text{M} \rightarrow 2\text{H} + \text{M}$
 - Ionization: $\text{Ar}^0 + e^- \rightarrow \text{Ar}^+ + e^- + e^-$
- Ionizing Breakdown in 6kV Potential
- Electrons Flow from Cathode \rightarrow Anode
- Inelastic MCC with Background
- Potential Function of e^- and Ar^+
- Merge Retains Features and Magnitude

While Controlling Computational Cost





HIGHER ORDER MOMENT CONSERVATION

- Moments defined as Integrals of VDF: $\bar{Q} = \int Q n f d v_i$
- Discrete Version: $n f \rightarrow w^{(p)} \delta(v^{(p)})$ such that $\bar{Q} = \sum w^{(p)} Q / \sum w^{(p)}$
- Merged Particles have 4 DOF each: w, v_x, v_y, v_z
- Number of Moments Conserved from Number of DOF

Moment	Order	

Cartesian Moments



HIGHER ORDER MOMENT CONSERVATION

- Moments defined as Integrals of VDF: $\bar{Q} = \int Q n f dv_i$
- Discrete Version: $n f \rightarrow w^{(p)} \delta(v^{(p)})$ such that $\bar{Q} = \sum w^{(p)} Q / \sum w^{(p)}$
- Merged Particles have 4 DOF each: w, v_x, v_y, v_z
- Number of Moments Conserved from Number of DOF

Moment	Order	
Mass	0 th	$\sum w^{(p)} = \bar{w}$
Mass Flux	1 st	$\sum w^{(p)} v_i^{(p)} = \bar{w} \cdot \bar{v}_i$

1 Particle - Mass & Momentum

Cartesian Moments

$$\bar{w} \text{ \& \; } \begin{bmatrix} \bar{v}_x \\ \bar{v}_y \\ \bar{v}_z \end{bmatrix}$$



HIGHER ORDER MOMENT CONSERVATION

- Moments defined as Integrals of VDF: $\bar{Q} = \int Q n f dv_i$
- Discrete Version: $n f \rightarrow w^{(p)} \delta(v^{(p)})$ such that $\bar{Q} = \sum w^{(p)} Q / \sum w^{(p)}$
- Merged Particles have 4 DOF each: w, v_x, v_y, v_z
- Number of Moments Conserved from Number of DOF

Moment	Order	
Mass	0 th	$\sum w^{(p)} = \bar{w}$
Mass Flux	1 st	$\sum w^{(p)} v_i^{(p)} = \bar{w} \cdot \bar{v}_i$
Momentum Flux	2 nd	$\sum w^{(p)} v_i^{(p)} v_i^{(p)} = \bar{w} \cdot \overline{v_i v_i}$

2 Particles - Mass, Momentum, and Diagonal 2nd: \bar{P}

Cartesian Moments

$$\begin{bmatrix} \overline{v_x v_x} & \overline{v_x v_y} & \overline{v_x v_z} \\ \overline{v_x v_y} & \overline{v_y v_y} & \overline{v_y v_z} \\ \overline{v_x v_z} & \overline{v_y v_z} & \overline{v_z v_z} \end{bmatrix}$$



HIGHER ORDER MOMENT CONSERVATION

- Moments defined as Integrals of VDF: $\bar{Q} = \int Q n f dv_i$
- Discrete Version: $n f \rightarrow w^{(p)} \delta(v^{(p)})$ such that $\bar{Q} = \sum w^{(p)} Q / \sum w^{(p)}$
- Merged Particles have 4 DOF each: w, v_x, v_y, v_z
- Number of Moments Conserved from Number of DOF

Moment	Order	
Mass	0 th	$\sum w^{(p)} = \bar{w}$
Mass Flux	1 st	$\sum w^{(p)} v_i^{(p)} = \bar{w} \cdot \bar{v}_i$
Momentum Flux	2 nd	$\sum w^{(p)} v_i^{(p)} v_j^{(p)} = \bar{w} \cdot \bar{v}_i \bar{v}_j$

3 Particles - Mass, Momentum, Full 2nd: \bar{P} & τ_{ij}

Cartesian Moments

$$\begin{bmatrix} \bar{v}_x \bar{v}_x & \bar{v}_x \bar{v}_y & \bar{v}_x \bar{v}_z \\ \bar{v}_x \bar{v}_y & \bar{v}_y \bar{v}_y & \bar{v}_y \bar{v}_z \\ \bar{v}_x \bar{v}_z & \bar{v}_y \bar{v}_z & \bar{v}_z \bar{v}_z \end{bmatrix}$$



HIGHER ORDER MOMENT CONSERVATION

- Moments defined as Integrals of VDF: $\bar{Q} = \int Q n f dv_i$
- Discrete Version: $n f \rightarrow w^{(p)} \delta(v^{(p)})$ such that $\bar{Q} = \sum w^{(p)} Q / \sum w^{(p)}$
- Merged Particles have 4 DOF each: w, v_x, v_y, v_z
- Number of Moments Conserved from Number of DOF

Moment	Order	
Mass	0 th	$\sum w^{(p)} = \bar{w}$
Mass Flux	1 st	$\sum w^{(p)} v_i^{(p)} = \bar{w} \cdot \bar{v}_i$
Momentum Flux	2 nd	$\sum w^{(p)} v_i^{(p)} v_j^{(p)} = \bar{w} \cdot \bar{v}_i \bar{v}_j$
Energy Flux	3 rd	$\sum w^{(p)} v_i^{(p)} (v^{(p)})^2 = \bar{w} \cdot \overline{v_i v^2}$

Cartesian Moments

$$\begin{bmatrix} \overline{v^2 v_x} \\ \overline{v^2 v_y} \\ \overline{v^2 v_z} \end{bmatrix}$$

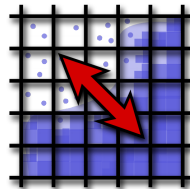
4 Particles - Mass, Momentum, Full 2nd, Energy Flux: q_i



EXTENSION TO HYBRID METHODS

Merge Quantities Needed for Hybridization:

- Reconstructed VDF Natural extension to Fokker-Planck/Boltzmann Solvers
- Higher Moment Merges would Facilitate extension to Hybrid Euler, Navier-Stokes, 13-moment, and Beyond
- Reversal of VDF/Moments to Particles would Enable Particle Generation in Transition Zones





END



Thank You

Questions?